3. Alkenone-Based Estimates of Past CO_2 Levels: A Consideration of Their Utility Based on an Analysis of Uncertainties

K.H. Freeman and M. Pagani

3.1 Introduction

Several molecular-based isotopic methods are employed for the reconstruction of past CO_2 levels. The focus in this chapter is on the use of organic materials derived from marine phytoplankton, in particular the lipid biomarkers called "alkenones" derived from haptophyte algae. These compounds are known to be useful for [CO_2] and temperature reconstructions; they have the added advantages of a high potential for preservation in marine sediments and ubiquity in the modern ocean. The latter property has enabled their study under a variety of marine conditions.

A number of comprehensive reviews give in-depth coverage of isotope fractionation by marine algae: in particular, Laws et al. (2001), who discuss carbon isotope fractionation by algae in general and provide a detailed consideration of fractionation by *Emiliania huxleyi*, which is the most cosmopolitan alkenone-producing species in the modern ocean. Pagani (2002) advances the Laws et al. review with more recent data and addresses in particular alkenone-based CO_2 estimates from ancient records. Hayes (2001) provides a detailed review of the fractionation of the isotopes of carbon during metabolic reactions. Included in his work is a discussion of carbon isotope fractionation during carbon fixation by organisms that employ the Calvin cycle, such as most marine algae. Freeman (2001) provides a general review of the isotopic biogeochemistry of organic matter in the modern ocean, which includes modern controls on the ^{13}C content

of inorganic carbon, and the influence of heterotrophic and photosynthetic effects on the ^{13}C abundance of organic carbon.

The theory and observations that are invoked in the calculations of ancient CO_2 levels are reviewed below:in particular, the uncertainties in the observed properties employed and the limitations imposed by the assumptions inherent in the method. To guide the reader in a practical application of these topics, also included is an analytical treatment of the propagation of errors for calculations related to CO_2 estimates, along with an example of these calculations based on previous works and showing that relative uncertainties are about 20% for Miocene CO_2 reconstruction based on alkenone $\delta^{13}C$ data. Also discussed below is the interpretation of isotopic data in the study of climate on longer timescales, including two examples from the Paleozoic.

3.2 Fractionation of Carbon Isotopes During Photosynthesis

The fixation of CO_2 by marine algae can be represented (Francois et al. 1993; Hayes 2001) by the flow of carbon into and out of the cell, and the flow of carbon taken up by enzyme-catalyzed fixation reactions. In Fig. 3.1, the flux of carbon that flows into and out of the cell is represented by ϕ_{in} and ϕ_{out}, respectively, while the flux of carbon fixed into carbohydrate is represented by ϕ_{fix}.

From mass balance,

$$\phi_{in} = \phi_{fix} + \phi_{out} \tag{3.1}$$

and the fraction of entering carbon that is fixed is represented by *f*, where

$$f = \phi_{fix}/(\phi_{fix} + \phi_{out}) = \phi_{fix}/\phi_{in} \tag{3.2}$$

Fractionation resulting from the combined effects of transport and fixation is represented as ε_P:

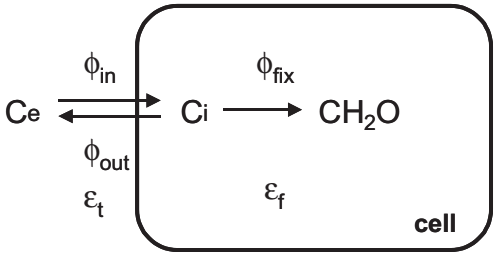

Figure 3.1. Schematic representation of carbon flow during marine photosynthetic carbon fixation. See text for definition of terms.

$$\varepsilon_P = 10^3 [(\delta_{CO2aq} + 1000)/(\delta_{org} + 1000) - 1] \sim \delta_{CO2aq} - \delta_{org} \quad (3.3)$$

where δ_{CO2aq} is the carbon isotopic composition of dissolved CO_2, and δ_{org} represents the ^{13}C content of organic carbon in the whole cell (Popp et al. 1989; Freeman and Hayes 1992). Based on mass balance considerations, ε_P can be expressed as a function of the relative amount of carbon fixed, and the isotope effects associated with transport (ε_t) and fixation (ε_f):

$$\varepsilon_P = \varepsilon_f - f(\varepsilon_f - \varepsilon_t) \quad (3.4)$$

Thus, total isotopic discrimination (ε_P) is greatest and approaches fractionation during the enzymatic fixation reaction (ε_f) when a small portion of incoming carbon is fixed. Total fractionation is small and approaches fractionation during transport (ε_t) when most of the carbon entering the cell is fixed into organic carbon (i.e., $f \rightarrow 1$). The ratio of carbon fixed relative to incoming carbon (f) is influenced by a multitude of factors, and it is the primary focus of many field and laboratory studies (e.g., Francois et al. 1993; Laws et al. 1995; Rau, Riebesell, and Wolf-Gladrow 1996; Popp et al. 1998; Burkhardt, Riebesell, and Zondervan 1999; Laws et al. 2001).

3.2.1 Controls on the Relative Amount of Carbon Fixed

In general, the rate of inorganic carbon fixed is a function of the concentration of available carbon and cellular growth rate. The cell is separated from its external environment by the cell membrane, or plasmalemma. The permeability of the membrane with respect to CO_2 is, to a large extent, proportional to its surface area (Laws et al. 1995; Laws, Bidigare, and Popp 1997). If the concentration of ambient dissolved carbon dioxide exceeds demand and/or the organism lacks the ability to actively increase the availability of carbon, then the supply of dissolved carbon dioxide is controlled by diffusion, with a flux that is proportional to the concentration gradient across the membrane (Farquhar et al. 1989). Leaking of carbon back to the external environment, as well as the demand for fixed carbon by the growing cell, will deplete the intracellular pool of dissolved carbon (c_i). Growth rates can be limited by a variety of factors, especially nutrient concentrations and light availability. Growth rates are typically reported in units of per day (day^{-1}) and must be scaled by the amount of organic carbon within the cell (which is proportional to its volume; Verity et al. 1992; Popp et al. 1998) in order to reflect the change in mass per unit time. Thus the demand for carbon is proportional to both growth conditions and the size and shape of the cell.

In summary, if carbon is diffusively transported across the cell membrane, then the fraction of carbon fixed relative to the incoming flux (f) is proportional to the concentration of CO_2 outside the cell (c_e), the growth rate of the cell (μ),

the quantity of organic carbon of the cell (C), and the permeability of the membrane with respect to CO_2 (P):

$$f = \phi_{fix}/\phi_{in} = \mu C/Pc_e \tag{3.5}$$

This equation (modified from Laws et al. 2001; Hayes 2001) assumes that carbon enters and exits by diffusion across the cell membrane and that the relative fluxes are driven by the concentration gradient across the membrane. In addition, it assumes that the carbon isotopic discrimination related to transport (as well as the resistance to transport across the cell membrane) is similar for the flow of CO_2 into and out of the cell.

The parameters that influence f can be substituted such that the cell volume (V) serves as a proxy for the amount of carbon in the cell (C), and the cell surface area (A) is used to approximate the permeability of the cell membrane (P). Thus the equation for fractionation during photosynthesis can be recast in terms of parameters that are more readily measurable in laboratory studies:

$$\varepsilon_P = \varepsilon_f - (\varepsilon_f - \varepsilon_t)(V/S)(\mu/c_e) \tag{3.6}$$

with the term V/S representing the ratio of cell volume to cell surface area (Popp et al. 1998).

This formulation emphasizes the influence of three fundamental controls on carbon isotopic fractionation by marine algae: (1) the concentration of carbon dioxide outside the cell, (2) the availability of a growth-limiting property, and (3) specific cell qualities, especially volume and surface area. Thus in field or culture studies, one might expect (and indeed observe) differences among species that reflect both the size and the shape of algal cells (Popp et al. 1998; Pancost et al. 1997). Further, one would expect significant control for a given species by both carbon concentrations and the availability of nutrients and/or light in the growth environment. The influence of carbon dioxide concentrations is, of course, of particular concern to those interested in paleoclimate reconstructions. However, growth conditions and cell geometry cannot be ignored in studies of ancient climate, and this continues to provide the biggest challenge to such applications.

In field studies of marine algae, growth rates and cell geometries can be difficult to characterize, and, further, older data sets rarely include these parameters. Thus Rau et al. (1992) and Bidigare et al. (1997) proposed the folding in of growth properties into a single term (b):

$$\varepsilon_p = \varepsilon_f - b/c_e \tag{3.7}$$

The term b represents all influences on ε_p other than CO_2(aq) concentrations and fractionation during enzymatic fixation.

3.2.2 The Problem of Active Transport

In the preceding discussion, it is assumed that carbon moves across the cell membrane by diffusion only. From a geological perspective, CO_2 concentrations in the modern ocean are low and possibly have been low for the past 25 million years or more (Pagani, Arthur, and Freeman 1999a) relative to past warm periods (Berner and Kothavala 2001). Thus it is not surprising that many modern algae can actively enhance the concentration of intracellular carbon dioxide as CO_2 concentrations become limiting to growth. Such carbon concentrating mechanisms (CCM) are inducible (Sharkey and Berry 1985; Laws, Bidigare, and Popp 1997) under low CO_2(aq) concentrations and involve active transport and/or CO_2 enhancement by way of enzymatic conversion of HCO_3^- into CO_2(aq). Laws et al. (1997) suggested that cells adjust the mechanism of transport (active vs. diffusion) in order to minimize energy costs associated with the demands of active transport. Accordingly, they propose a nonlinear model, where fractionation (ε_P) is a function of the relative amount of carbon delivered to the cell by active means. Keller and Morel (1999) propose a similar mathematical model, which can account for the uptake of either bicarbonate or aqueous CO_2. Based on available isotopic data, Laws et al. (2001) suggest aqueous CO_2 is the likely substrate for active transport.

Although active transport has been associated with lower ε_P values, Laws et al. (2001) emphasize that they are not diagnostic of its presence. In particular, a decrease in ε_p due to the use of ^{13}C-enriched bicarbonate can be offset by an increase in the flux of carbon into the cell such that the ratio of fixed to incoming carbon (*f*) decreases. For the purposes of ancient climate reconstruction, active transport poses a difficult problem, since it can decouple isotopic fractionation from carbon availability. In studies of past CO_2, the authors seek biomarkers for a taxonomic group for which active transport is unlikely. For example, laboratory evidence suggests that neither active transport, nor a carbon concentrating mechanism, nor calcification are significant influences on ε_p of certain haptophyte algae and that the diffusion model is appropriate (Bidigare et al. 1997; Nimer, Iglesias-Rodriguez, and Merrett 1997; Sikes, Roer, and Wilbur 1980), at least under conditions similar to the modern and near-recent ocean. However, when one is working on very long timescales, modern analogs of ancient species are less common; thus an assumption of biological uniformitarianism becomes increasingly risky. Under these circumstances, paleo-CO_2 research requires the assumption that past CO_2 levels were sufficiently high such that a carbon concentrating mechanism was not required, or that the ratio of active to diffusive carbon transport was relatively invariant.

3.2.3 Isotopic Biogeochemistry of Alkenone-Producing Organisms

Alkenones are long-chain ketones (Fig. 3.2) derived from a species of haptophyte algae (Marlowe et al. 1984).

Most notably, they are produced by *Emiliania huxleyi* (Volkman et al. 1980), which is found throughout the modern ocean (Westbroek et al. 1993) and *Geo-*

−1
0
+1

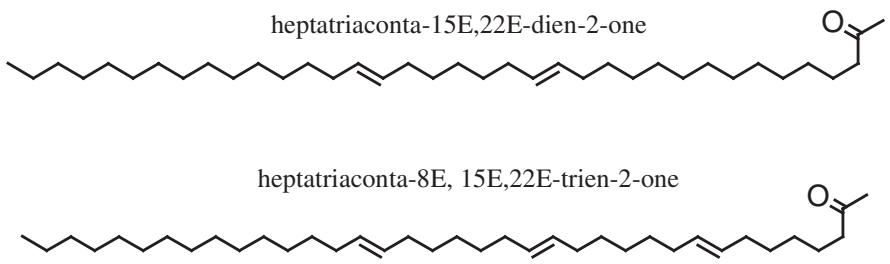

Figure 3.2. The molecular structures of $C_{37:2}$ and $C_{37:3}$ alkenones.

phyrocapsa oceanica (Volkman et al. 1995). The most commonly observed structures are the C_{37}, C_{38}, and C_{39} methyl and ethyl ketones (de Leeuw et al. 1980), with heptatriaconta-15E,22E-dien-2-one ("$C_{37:2}$ alkenone") and heptatriaconta-8E, 15E,22E-trien-2-one ("$C_{37:3}$ alkenone") most often employed in sediment studies because of their utility in paleotemperature reconstructions (e.g., Brassell et al. 1986; Reviewed by Brassell 1993; Sachs and Lehman 1999).

Rechka and Maxwell (1988a, b) confirmed the *trans* configuration of the double bonds and suggested this property makes them more resistant to biological degradation. Indeed, they are more refractory than other lipids in marine waters and sediments (Wakeham et al., 1997a; 1997b, 2002); there is, however, evidence that under certain conditions, the more unsaturated forms may be lost preferentially (Freeman and Wakeham 1992; Gong and Hollander 1999).

Alkenones have attracted a great deal of attention from paleoceanographers. There are many field and laboratory studies of the temperature dependence of the relative abundance of $C_{37:2}$ and $C_{37:3}$ alkenones (Brassell 1993; Herbert 2001), as well as their isotopic properties. For purposes of reconstructing ancient CO_2 levels, alkenones are perhaps the most popular choice because of their ubiquity, preservation, and taxonomic specificity. In addition, as noted above, alkenone-producing haptophytes apparently do not employ active transport mechanisms at the CO_2 concentrations found in the oceans today, allowing the application of equations 4 and 6.

3.2.4 Laboratory Observations

The isotopic properties of alkenones and their source organisms are documented in numerous laboratory experiments that use a nitrate-limited continuous culture system called a chemostat. The chemostat system permits investigators to control growth rates by regulating the supply of a limiting nutrient (e.g., nitrate) and to perform experiments under steady-state conditions. The method has been successfully applied to evaluate the relationship between ε_p, c_e, μ, and cell geometry (reviewed by Laws et al. 2001), for haptophytes *Emiliania huxleyi* (Bidigare et al. 1997) and *Isochrysis galbana* (Laws et al. 2001), as well as the diatoms *Phaeodactylum tricornutum* (Laws, Bidigare, and Popp 1997) and *Porosira gla-*

−1
0
+1

cialis (Popp et al. 1998) among others. Light- and temperature-limited growth of *E. huxleyi* using a turbidostat (Rosenthal et al. 1999) gives similar response to the nitrate-limited growth found in the chemostat experiments, with a linear relationship between ε_p and μ/c_e.

The more common and traditional methodology involves batch cultures grown in a medium containing nutrients in excess required for growth. Although batch cultures are sensitive to initial conditions, they can be effective in isotopic studies, provided carbon is harvested while cell densities are low to prevent self-shading and to prevent substantial changes in the inorganic carbon pools (Hinga et al. 1994). Unfortunately, there is an unresolved difference between the results from chemostat experiments and some dilute, light-limited but nitrate-replete batch cultures. Batch experiments results record overall lower values for ε_p, and nonlinear relationships between ε_p and μ/c_e, and this may indicate that the regulation of carbon uptake is influenced by the abundance of nitrate or possibly other nutrients (Burkhardt, Riebesell, and Zondervan 1999; Riebesell et al. 2000a), or it may reflect differences in isotopic systematics between stationary (chemostat) and exponential (batch cultures) growth phases. However, the specific cause for the differences among various batch experiments, and between continuous culture and batch cultures, is unresolved and remains an area for further investigation (Laws et al. 2001).

Culture studies are useful to evaluate intermolecular isotopic variations. For studies of continuous culture, alkenones are, on average, 3.9‰ ($\sigma = 0.8$) depleted relative to whole cells (Laws et al. 2001). Values reported for batch cultures (Riebesell et al. 2000b) are slightly more depleted and average -5.2 ($\sigma = 0.3$), with the combined data set (continuous culture + batch) giving an average $\Delta\delta$ value of -4.5 ($\sigma = 0.8$). This value is close to the value used by Jasper et al. (1994), -3.8‰; and it is generally consistent with observed depletion of linear lipids from whole biomass of 3 to 4‰ (Hayes 1993; Schouten et al. 1998). In general, field-based studies of alkenones assume an invariant $\Delta\delta$ value of 4‰; (Bidigare et al. 1997; Jasper et al. 1994). As reviewed by Hayes (2001), the isotopic composition of an individual cellular component can be influenced by changes in the flux of carbon to various fates within the cell, and thus there is a prospect for $\Delta\delta$ values to be sensitive to conditions in the growth environment. Subtle variations in growth conditions could potentially explain the range in observed values of $\Delta\delta$ as well as the approximate 1‰ difference observed between continuous and batch culture experiments.

Laboratory results have helped to determine the fractionation of carbon isotopes associated with enzymatic fixation (ε_f). In vitro results with ribulose-1,5-bisphosphate caroxylase/oxygenase (Rubisco) document values of 30–29‰; for eukaryotes, and lower values (22–18‰) for the bacterial form of Rubisco (Guy, Fogel, and Berry 1993; Roeske and O'Leary, 1985). Microaglae have, in addition to Rubisco, a small activity of β-carboxylase enzymes that attenuate the net fractionation. Chemostat data suggest the combined enzymatic value is around 25‰ for haptophytes, and this value is generally consistent with field observations (Bidigare et al. 1997; Popp et al. 1998). As discussed by Goericke and

Fry (1994) et al. (1994), a range of values is possible, depending on relative enzyme activities, with 25‰ corresponding to approximately 10% β-carboxylase activity. A lower activity would lead to a greater value for ε_f, and Goericke and Fry (1994) et al. (1994) calculate a possible range of 25–28‰. A range of values was observed in the chemostat experiments of Bidigare et al. (1997) for *E. huxleyi,* and calculations incorporating the 95% confidence limits of these data yeild 25–27‰; for ε_f (Pagani et al. 1999a).

3.2.5 Field Observations

Bidigare et al. (1997; 1999a) compiled alkenone-based measurements of ε_p to evaluate relationships between ε_p, growth conditions, and observed concentrations of CO_2(aq). Laws et al. (2001) and Pagani (2002) have enlarged the data set with the inclusion of more recent studies (Popp et al. 1999; Eek et al., 1999; Laws et al., 2001); in total, the observations are drawn from environments that span the ocean and the spectrum of nutrient availability (Fig. 3.3). Values for b are calculated from equation 7, using ε_p values determined from $\delta^{13}C$ values of alkenones and CO_2(aq). We present the b values calculated using ε_f = 26‰; to represent the median in the range of values estimated from the chemostat results noted in the preceding discussion. The calculations assume an isotopic difference between biomass and alkenones of 4‰.

The range of values for b reflect the influence of factors other than the concentration of carbon dioxide, principally cell geometry (V/S) and growth rate (μ), on the expression of ε_p. Importantly, this data set represents isotopic characteristics of only alkenone-producing haptophyte algae, thus most probably minimizing the influence of cell geometry. It is proposed, therefore, that the parameter b represents largely the influence of growth rate. Bidigare et al. (1997) showed that this approach is consistent with growth rates measured in the field and that it is generally consistent with continuous-culture laboratory experiments employing both calcifying and noncalcifying strains of *E. huxleyi*. Unfortunately, most of the field studies that constitute this compilation did not include direct measurements of growth rates because this procedure is difficult to do in the field. Thus, the link between growth rates and values for b is based on the correlation between b and the measured concentration of phosphate in the same samples (Fig. 3.3).

The strong correlation between b and PO_4^{3-} is less than compelling, however, when one considers that phosphate concentrations are generally too high to be growth limiting in most of the samples (Bidigare et al. 1997). Nevertheless, the strong correlation suggests that some growth-limiting property is proxied by the phosphate measurements, such as a trace element that serves as a micronutrient (Bidigare et al. 1997).

Both Laws et al. (2001) and Pagani (2002) discuss the relationship between phosphate and b in detail, with consideration of additional controls. For example, as shown in Fig. 3.4A, there is some correlation between phosphate and CO_2 concentrations, which influences the relationship with b values. Correlations

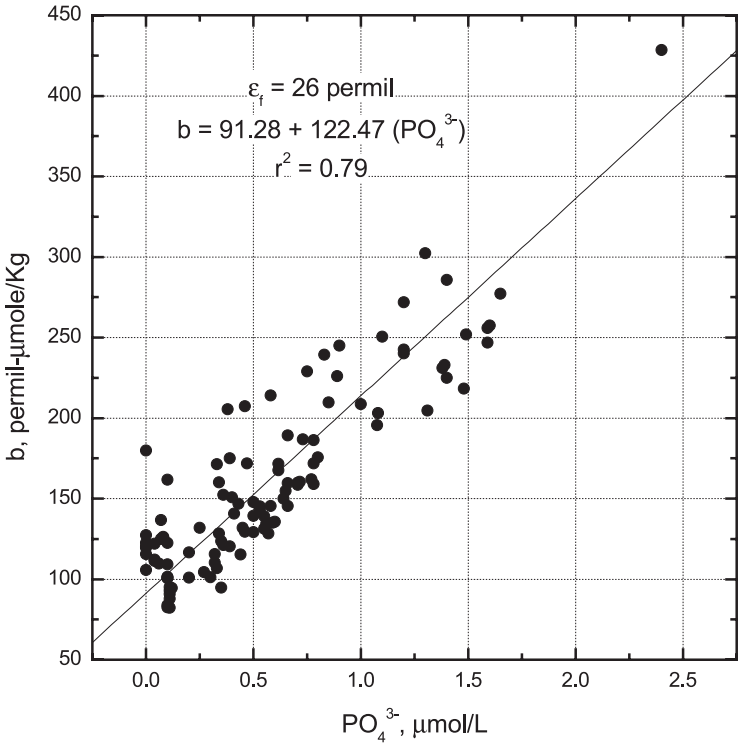

Figure 3.3. Alkenone-based estimates of b plotted as a function of observed PO_4^{3-} concentrations. Data are taken from values compiled by Pagani (2002), with ε_f = 26‰.

between ε_p values and either phosphate (r^2 = 0.23) and CO_2(aq) (r^2 = 0.1) are obviously not as strong as the correlation between ε_p and PO_4^{3-}/CO_2(aq), where r^2 = 0.31 (Fig. 3.4B,C). Although there is a visible trend in Fig. 3.4C, there remains significant variation in ε_p that is not accounted for by the PO_4^{3-}/CO_2(aq) ratio and it is possible that other factors in the growth environment (temperature, light quality, etc.) or cell geometry are important in the open-ocean photic zone. Exact controls on isotopic fractionation continue to be debated, and future field and laboratory studies will likely shed further light on the chemical and biological controls on ε_p in modern waters.

3.2.6 A Sediment Test of the Alkenone Method

In the modern ocean, phosphate concentrations are more highly correlated to alkenone-derived ε_p values than other factors, including CO_2(aq). Although a range of CO_2 concentrations exists in surface waters today, it is relatively narrow, which reflects the fact that ocean surface waters approach (but do not reach) chemical and isotopic equilibrium with the atmosphere (reviewed by Freeman,

−1
0
+1

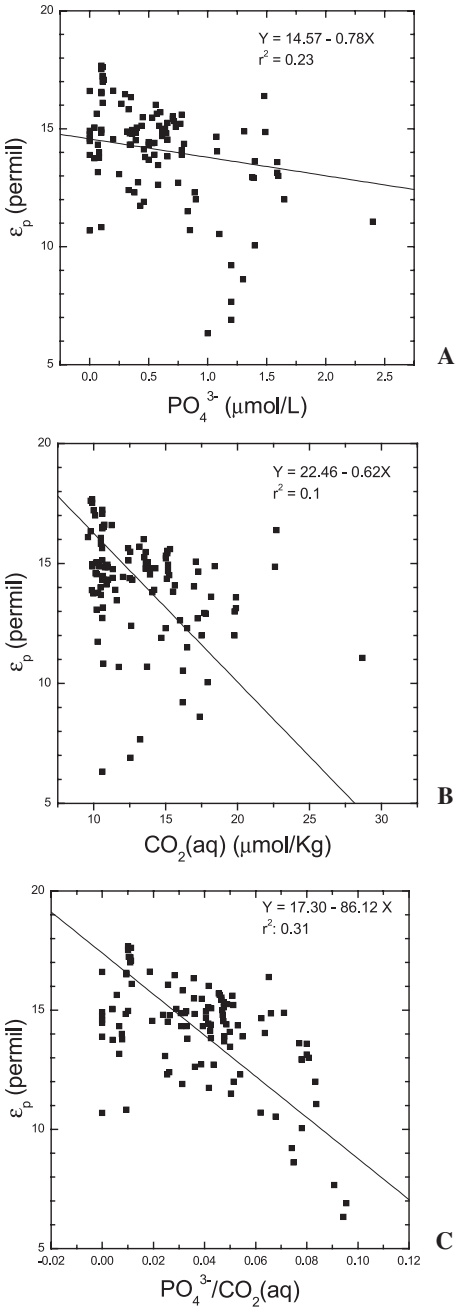

Figure 3.4. Cross plots of ε_p values with phospate concentrations (A), aqueous carbon dioxide (B), and the ratio of phosphate to carbon dioxide (C). All lines represent geometric mean regressions (Sokal and Rohlf 1995).

____−1
____ 0
____+1

2001). In order to test the influence of CO_2 on ε_p values, one is forced to exploit laboratory studies, which may or may not reconstruct natural conditions adequately (Laws et al. 2001). An alternative approach is to look to the sedimentary record of recent atmospheric changes.

We recently (Pagani et al. 2002) tested the relationship proposed from alkenones in modern ocean waters by using samples collected from sediments along a transect in the central Pacific Ocean. The depth of alkenone production was inferred from temperatures estimated based on the unsaturation ratio of alkenone abundances (Uk_{37}' values; Ohkouchi et al. 1999), and we employ these depth estimates to determine phosphate values along with both the concentration and $\delta^{13}C$ values of dissolved CO_2. Based on measured inorganic carbon and alkenone $\delta^{13}C$ values, water-column phosphate concentrations at the depth of alkenone synthesis, and the relationship expressed in Fig. 3.3, we calculated $CO_2(aq)$ concentrations at the time of alkenone production.

Alkenone-based $CO_2(aq)$ values were consistently lower than concentrations observed in the modern ocean. However, this difference can be largely accounted for by the removal of anthropogenic contributions from modern values. The resulting match is strong: 84% of the alkenone-based estimates fall within 0–20% of the preindustrial water-column values. A subset of these results is shown in Fig. 3.5, which represents estimates based on water-column data collected in the spring.

The strength of this agreement suggests that the empirical relationship between b and phosphate derived from a wide variety of oceanographic environments (including high- and low-phosphate concentrations) can be used to reconstruct ancient CO_2 levels from alkenone $\delta^{13}C$ values, provided an estimate of paleophosphate concentration or a reasonable range of values are available. It further supports earlier findings that the isotopic composition of alkenone-producing haptophytes is not substantially affected by the active transport of inorganic carbon or calcification. This is promising news for efforts to reconstruct greenhouse gas variations in the past.

3.3 Alkenone-Based Estimates of Ancient CO_2 Levels

3.3.1 Measured Properties in the Calculation of Ancient CO_2 Levels

When employing alkenones for ancient CO_2 reconstructions, the rearranged form of Equation 3.7 is employed:

$$c_e = (\varepsilon_f - \varepsilon_p)/b \tag{3.8}$$

Although this equation contains only three variables, they represent a large number of observations and underlying calculations. The observed and derived properties are listed in Table 3.1, along with our estimate of the approximate uncertainty in the value and the primary basis for each error estimate.

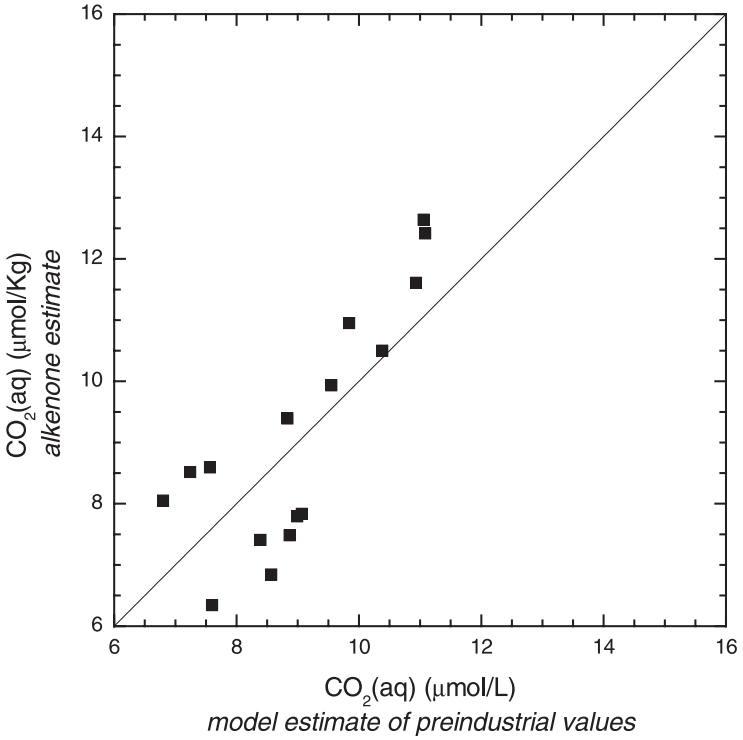

Figure 3.5. Cross plot of the estimated preindustrial CO_2 in western Pacific waters (from Pagani et al. 2002). The ordinate represents values based on alkenone measurements; the abscissa represents values determined from measurements in modern waters minus an estimated contribution of anthropogenic carbon. The estimate of anthropogenic CO_2 is based on the Geophysical Fluid Dynamics Laboratory's Modular Ocean Model (Pacanowski et al. 1991). Values plotted are based on spring production data. Dashed line represents a 1:1 correlation.

Values for ε_p are based on the isotopic difference between an estimate of the $\delta^{13}C$ values of the organic matter produced by ancient algae ($\delta^{13}C_{org}$) and the coexisting dissolved CO_2 in the photic zone ($\delta^{13}C_{carb}$) as noted earlier and defined in Equation 3.3. The value for $\delta^{13}C_{org}$ is determined by adding 4‰ to the measured value of the $C_{37:2}$ alkenone extracted from the ancient marine sediment. This correction reflects lipid-biomass isotopic differences ($\Delta\delta$) discussed previously and is consistent with values employed by other researchers and in our earlier CO_2 reconstructions (Pagani et al. 1999a, b). We have selected the median of the estimate for ε_f (= 26‰) derived from chemostat culture studies as discussed previously, giving an uncertainty of 1‰.

The isotopic composition of carbon dioxide in the ancient growth environment is determined from measurements of a selected carbonate phase known to derive

Table 3.1. Properties involved in estimating ancient CO_2 concentrations and the nature and sources of their respective error estimates

Property	Source	Approx. Error	Basis for Error Estimate
$\delta^{13}C_{carb}$	Foraminifera or some other planktonic carbonate phase	0.2‰	Analytical
$\delta^{13}C_{org}$	$\delta^{13}C$ of $C_{37:2}$ alkenones + 0.4‰	1.0‰	Analytical; culture studies
Temperature	$\delta^{18}O$ of planktonic carbonate source	3°C	Analytical (0.1‰), estimated uncertainty in SMOW
Phosphate	Estimated from ocean or sediment properties	0.1 μMol/kg	Best guess
b values	Field data	20%	Regression statistics
ε_f	Lab studies	1.0‰	Available data

from the photic zone in the upper water column, such as single species or genera of planktonic foraminifera (Pagani et al. 1999a). The carbonate values are used to calculate $\delta^{13}C$ values of CO_2(aq) in equilibrium with the carbonate phase, based on isotopic relationships determined by Romanek, Grossman, and Morse (1992) and Mook, Bommerson, and Staberman (1974) and as detailed in the papers by Freeman and Hayes (1992) and Pagani et al. (1999a). For example, combining the equations of Romanek et al. (1992) and Mook et al. (1974), $\delta^{13}C$ values for dissolved CO_2 are calculated by the following equation:

$$\delta^{13}C_{co2aq} = 373/T + 0.19 + \delta^{13}C_{carb} - 11.98 + 0.12T \quad (3.9)$$

where T is temperature in kelvin.

This calculation requires an estimate of ancient sea surface temperatures, which are typically evaluated using the measured $\delta^{18}O$ values of the planktonic carbonate phase. The temperature estimates require the $\delta^{18}O$ value of coexisting seawater (i.e., ancient SMOW), which can be difficult to determine and is the principle source of uncertainty in this aspect of the calculation. Analytical uncertainties in both carbon and oxygen isotopic measurements are small, approximately 0.2 and 0.1‰, respectively.

A detailed discussion for the strategy and methods for calculating ε_p from isotopic analyses of sedimentary alkenones is provided by Pagani et al. 1999a. In that work, we employed alkenones extracted from sediment samples, in concert with 250–354 and 354–420 μm size-fractionated planktonic foraminifera. The selection of larger foraminifera specimens is routine in isotopic studies in order to avoid isotopic effects associated with juvenile organisms. In addition, there are documented metabolic effects, for example, due to interactions with symbiont phototrophs, which can cause foraminiferal $\delta^{13}C$ values to deviate from equilibrium with the water column (Spero and DeNiro 1987; Spero and Lea

1993). These influences are typically less than 1.5‰, but if not accounted for, they will generally lead to an overestimation of CO_2 concentrations.

A value for b is the final variable required to determine ancient CO_2 levels. The term b is calculated from estimates of ancient phosphate concentrations and the regression shown earlier, in Fig. 3.3. Phosphate values can be estimated based on modern ocean properties in the near recent (i.e., Pagani et al. 2002) or from properties of the accumulated sediments. In this regard, it is recommended that researchers use samples from oceanographic sites that have experienced relatively stable nutrient conditions in the photic zone. Such sites include open gyre localities, where nutrient concentrations are low and stable. In the ancient record, linear accumulation of biogenic materials (e.g., Pagani et al. 1999a) provides strong evidence for nutrient stability over time. Multiple sites and records should be studied in order to dissect global signals from the influence of local conditions on an isotopic record from an individual site (Freeman 2001).

3.3.2 Propagation of Uncertainties

The propagation of errors in the calculation of ancient CO_2 levels can be carried out using basic equations for the handling of random errors, with the assumption that the errors are independent and Gaussian in distribution. In general, for a property, x, that is a function of more than one variable (u, v):

$$\sigma_x^2 = \sigma_u^2 \left(\frac{\partial x}{\partial u}\right)^2 + \sigma_v^2 \left(\frac{\partial x}{\partial v}\right)^2 + 2\sigma_{uv}^2 \left(\frac{\partial x}{\partial u}\right)\left(\frac{\partial x}{\partial v}\right) \tag{3.10}$$

The first two terms represent the sum of squares of individual uncertainties weighted by the squares of the partial derivatives of the function. The third term, when the errors of u and v are independent, becomes negligible and is typically ignored.

Taylor (1982) and Bevington and Robinson (1992) provide excellent discussions and examples of the application of error propagation. Readers with experience in analytical chemistry or physics will be most familiar with such an approach and the various error relationships derived from Equation 3.10. For example, the combined error for added or subtracted properties is simply the square root of the sum of the squares of the errors for the properties.

Equation 3.10 is used for the propagation of errors in Equation 3.8. Because errors are assumed to be independent, the final cross term is ignored. In order to simplify this presentation, we have combined the difference $(\varepsilon_f - \varepsilon_p)$ into a single term $\Delta\varepsilon$:

$$\sigma_{ce}^2 = \sigma_{\Delta\varepsilon}^2 \left(\frac{\partial(b/\Delta\varepsilon)}{\partial\Delta\varepsilon}\right)^2 + \sigma_b^2 \left(\frac{\partial(b/\Delta\varepsilon)}{\partial b}\right)^2 \tag{3.11}$$

Differentiating the terms in Equation 3.11 yields:

$$\sigma_{ce}^2 = \sigma_{\Delta\varepsilon}^2 \left(\frac{b}{\Delta\varepsilon^2}\right)^2 + \sigma_b^2 \left(\frac{1}{\Delta\varepsilon}\right)^2 \tag{3.12}$$

This equation forms the basis for the calculation of uncertainties discussed below.

3.3.3 Errors in Δε

$\Delta\varepsilon$ is calculated from the subtraction of ε_p from ε_f, and the cumulative error is the square root of the sum of the squares of the errors in each property:

$$\sigma_{\Delta\varepsilon}^2 = \sigma_{\varepsilon f}^2 + \sigma_{\varepsilon p}^2 \tag{3.13}$$

As noted above, we assume $\varepsilon_f = 26‰ \pm 1‰$. The uncertainty in values of ε_p is based on two terms (see Equation 3.3): the $\delta^{13}C$ values of dissolved CO_2 and organic carbon derived from phytoplankton. The error estimate for $\delta^{13}C_{org}$ values is based on both the analytical error in the isotopic measurements of alkenones (ca. 0.7‰; Pagani et al. 1999a; 0.4‰ Pagani et al. 2002) and the laboratory studies reporting about 4‰ lipid-biomass differences (0.8‰). Here we employ 0.6‰ for the error in the isotopic analysis of individual alkenones and 0.8‰ for the uncertainty in the intermolecular correction. Thus the error in $\delta^{13}C_{org}$ is the square root of the sum of the squares of these values, or 1‰.

Error determination for inorganic carbon is based on the combined errors for the temperature estimate (ca. 3°C) and the analytical uncertainty in the carbon isotopic measurements (0.2‰). The calculation is based on Equation 3.10, using Equation 3.9 as the differentiated function. Thus:

$$\sigma_{co2aq}^2 = \sigma_T^2 \left(\frac{\partial f}{\partial T}\right)^2 + \sigma_{carb}^2 \left(\frac{\partial f}{\partial \delta_{carb}}\right)^2 \tag{3.14}$$

where the terms σ_{co2aq}, σ_T, and σ_{carb} represent the uncertainties in the values for $\delta^{13}C$ of CO_2(aq), temperature, and $\delta^{13}C_{carb}$, respectively. The term δ_{carb} represents the $\delta^{13}C$ values of planktonic carbonate. The term f is the function used to calculate $\delta^{13}C_{co2aq}$ represented by Equation 3.9. Using this approach, differentiating Equation 3.9 in terms of both T and δ_{carb}, employing the error estimates listed in Table 3.1, and assuming T = 298K, we estimate an uncertainty of 0.4‰ for the $\delta^{13}C$ value of aqueous CO_2.

Based on the above calculations, we now calculate the uncertainty in the estimate of ε_p values:

$$\begin{aligned} \sigma_{\varepsilon p}{}^2 &= \sigma_{co2aq}{}^2 + \sigma_{org}{}^2 \\ &= (0.4)^2 + (1.0)^2 \\ \sigma_{\varepsilon p} &= 1.1‰ \end{aligned} \tag{3.15}$$

This value can be applied to Equation 3.13, and the error for $\Delta\varepsilon$ determined:

$$\begin{aligned}\sigma_{\Delta\varepsilon}{}^2 &= \sigma_{\varepsilon f}^2 + \sigma_{\varepsilon p}{}^2 \\ &= (1.0)^2 + (1.1)^2 \\ \sigma_{\Delta\varepsilon} &= 1.5‰\end{aligned} \tag{3.16}$$

The uncertainty for b is based on the standard error determined from regression statistics for the alkenone data set discussed earlier and presented in Fig. 3.3. This data set includes 109 pairs of values for b and phosphate determinations from a wide variety of localities in the modern ocean. The standard error is calculated as discussed by Sokal and Rohlf (1995):

$$\sigma_b = \sqrt{s_{yx}^2\left[1 + \frac{1}{n} + \frac{\left(x_i - \bar{x}\right)^2}{\Sigma x^2}\right]} \tag{3.17}$$

where

$$s_{yx}^2 = \left(\Sigma y^2 - \frac{\Sigma xy^2}{\Sigma x^2}\right)$$

and the properties Σy^2 and Σx^2 represent the sum of the squares of the deviations for each variable, with Σxy^2 representing the covariance (Sokal and Rolf, 1995). In the regression (shown in Fig. 3.3), x is represented by phosphate values, while y represents values for b. For values of phosphate ranging from 0.2 to 1 μmol/kg (using $\varepsilon_f = 26‰$), the error for b is 27.2‰-μmol/kg. Uncertainties based on the regression statistics increase for values for phosphate concentrations that are higher or lower than those in the calibration data set.

This represents an approximately 20% uncertainty derived from the regression of b versus phosphate concentrations from all available modern field observations. If ancient samples are from a locality for which a specific phosphate-b calibration is possible, it may reduce the magnitude of this uncertainty. For example, Popp et al. (1999) used a subset of the above data set for the Pacific Ocean and estimated approximately 3% uncertainty for the relationship derived from the regression of b and PO_4^{3-}. This resulted in an overall lower estimate of the uncertainty in the alkenone method for CO_2 reconstruction (ca. 11%).

By employing $\varepsilon_f = 26‰$, $\sigma_b = 27.2‰$ μmol/kg, and $\sigma_{\Delta\varepsilon} = 1.6‰$, we can use Equation 3.12 to calculate the uncertainty in estimated CO_2 concentrations for given values of b and ε_p. These values are presented as absolute uncertainty (in μmol/kg) in Fig. 3.6 and as a relative uncertainty (%) of calculated c_e estimates in Fig. 3.7.

The shaded regions represent values of b that correspond to a range of phosphate concentrations between 0.1 and 1.0 μmol/kg. As shown in these figures, the uncertainties in estimated ancient CO_2(aq) concentrations range between 20 and 30% for ε_p values below 20‰, and they increase dramatically with greater isotopic fractionation (ε_p). This increase represents the decreased sensitivity of

−1
0
+1

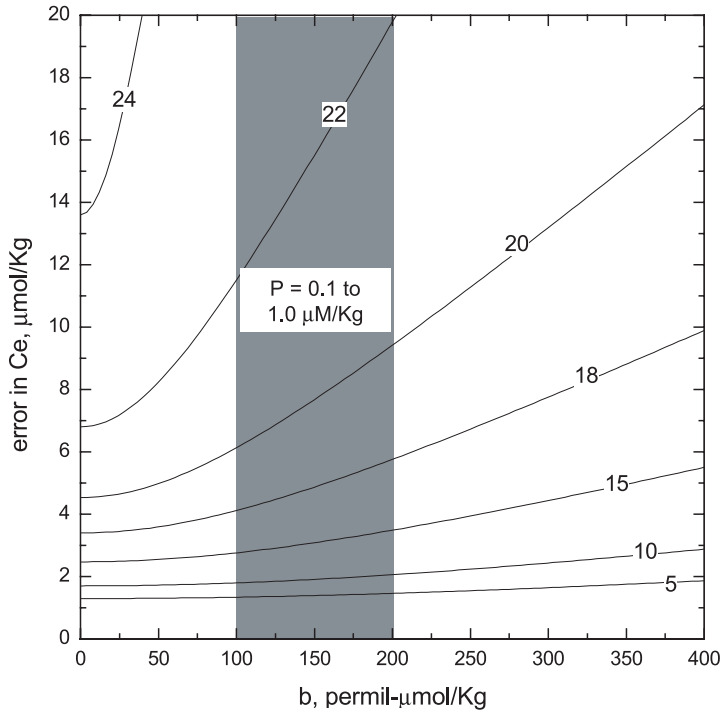

Figure 3.6. Calculated values of absolute uncertainties in estimates of dissolved CO_2 concentrations based on alkenone analyses. Shaded region represents the range of values of b corresponding to phosphate concentrations in the modern ocean. Contours represent ε_p values in units of ‰.

the technique at high CO_2 levels. Once CO_2 reaches higher than 8 to 10 times modern levels, carbon saturates fixation by algae, and, as noted in the discussion of Equation 3.4, $f<<1$, and $\varepsilon_p \rightarrow \varepsilon_f$.

When CO_2 levels are relatively constrained, isotopic analyses of alkenones and inorganic carbon can be used to evaluate changes in growth rates and, by association, changes in nutrient concentrations (Pagani, Arthur, and Freeman 2000; Bidigare et al. 1999b). A similar approach to error propagation can be invoked to estimate uncertainties in the reconstructed values. Although in this case, the uncertainty in the estimate will rely on how well one knows values for CO_2 concentrations in addition to the quality of the isotopic results.

3.3.4 The Problem with Phosphate

The observed relationship between b values and phosphate concentrations plays an important part in the proxy method for CO_2 reconstruction, while also serving as a major source of uncertainty in the results. Constraining phosphate concen-

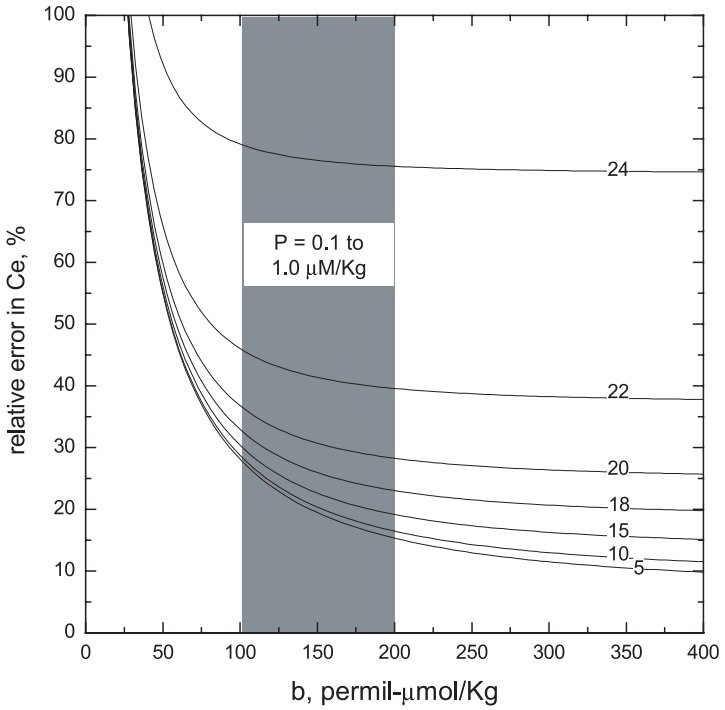

Figure 3.7. Calculated values of the relative uncertainties in estimates of dissolved CO_2 concentrations based on alkenone analyses. Shaded region represents the range of values of b corresponding to phosphate concentrations in the modern ocean. Contours represent ε_p values in units of ‰.

trations in the past is an additional challenge to this approach. In Fig. 3.8, we present a contoured plot of the value for dissolved CO_2 estimated from b for measured ε_p values.

The shaded regions represent the range in the concentrations of CO_2(aq) (horizontal region) and phosphate concentrations (vertical region) observed in the modern ocean. We note, however, that the range of phosphate concentrations could be significantly higher in upwelling regions (see Fig. 3.3), which can lead to values of b that are 300‰-μmol/kg or even higher.

The error in the estimated value of b (ca. 20%) from phosphate concentrations is relatively constant when concentrations of phosphate are within the range observed throughout much of the modern ocean (ca. 0.1–ca. 1 μmol/kg). However, this describes the uncertainty in the *relationship* between these properties based on the variance of phosphate and b measured in the modern ocean. Thus, for ancient studies, it is assumed that phosphate uncertainties are similar to that for modern phosphate values in the data set presented in Fig. 3.3. With good sample site selection, the variation in phosphate can be minimized, and the

−1
0
+1

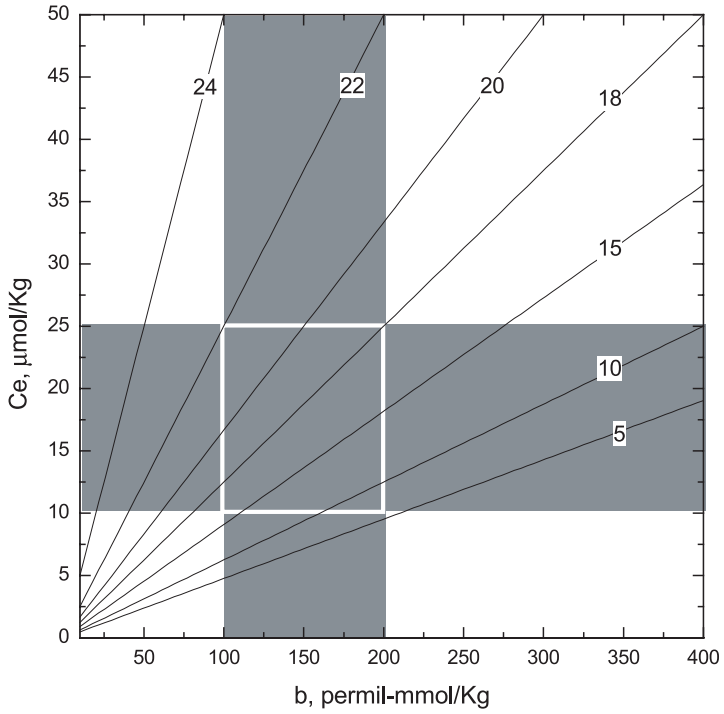

Figure 3.8. Contours of εp values represented estimates of dissolved CO_2 concentrations as a function of b values. The vertical shaded region respresents the range of values of b corresponding to phosphate concentrations in the modern ocean. The horizontal shaded region represents the general range in dissolved CO_2 concentrations observed in the modern ocean.

uncertainty in a paleo-PO_4^{3-} estimation may well be similar to that in the modern data set. In particular, it is essential that the researcher have some estimation of whether the location was characterized by enhanced nutrient concentrations through upwelling, runoff, or other mechanisms as opposed to a low nutrient environment, such as the subtropical gyres today. As noted above (and by Pagani et al. 1999a), the use of sediment accumulation characteristics is essential to sort out these possibilities. These two environmental extremes result in the range in phosphate concentrations shown in Fig. 3.3 (Popp et al. 1999). ε_p values in the modern ocean are relatively more sensitive to variations in phosphate concentrations than CO_2(aq) concentrations, since the latter are partially reset by equilibration with the atmosphere. The dominance of the isotopic signature by phosphate as observed in today's ocean is not likely true through time, since significant changes in atmospheric CO_2 levels in the past will ultimately dominate the record of ε_p variations over Earth's history (Hayes, Strauss, and Kaufman 1999).

____−1
____ 0
____+1

It clearly would be helpful to have a better tool for estimating phosphate values than relying on the averaged depositional condition for a given site. Popp et al. (1999) recommend the use of elemental ratios of Cd and Ca in calcite tests from planktonic foraminifera. This ratio is documented to vary with the abundance of phosphate in the modern ocean and may be a useful proxy for reconstructing phosphate concentrations in the ancient ocean (e.g., Boyle 1992; Oppo and Rosenthal 1994; Mashiotta, Lea, and Spero 1997). However, this relationship is not documented for timescales longer than the last glacial era, and there are observations that document a temperature effect (Rickaby and Elderfield 1999). Popp et al. (1999) estimate this approach could potentially provide a phosphate estimate with an uncertainty of about 10%. However, this estimate predated the discovery of the temperature effect, which has discouraged its use in such applications. Currently estimates of paleophosphate concentrations take into account past productivity based on sediment properties and accumulation along with reconstructed circulation and wind patterns. As noted below, these efforts can provide reasonable constraints on phosphate values, giving a range of estimated values.

3.3.5 Miocene Reconstructions

In our previously published CO_2 reconstructions for the Miocene based on alkenones (Pagani et al. 1999a, b), we estimated uncertainties by bracketing our estimates with minimum and maximum values for Equation 3.7. For example, we employed two phosphate values (0.2–0.3 μmol/kg), two values for ε_f (25 and 27‰), the maximum 95% confidence band, along with the geometric mean regression Equation in Fig. 3.3, to yield a range of CO_2 estimates. We considered DSDP site 588 in the southwestern Pacific to represent the sample locality with the greatest stability in terms of nutrient dynamics, although the range of CO_2 estimates was similar for all the sites. At DSDP site 588, the median CO_2 estimates ranged from about 280 to 200 ppmv, with the calculated maximum and minimum values ranging approximately ± 40 ppmv. By employing the error propagation approach presented here, we would raise the error estimate slightly, with uncertainty ranging between 40 and 56 ppmv (ca. $\pm$ 20%). This error is slightly higher than that calculated in an earlier publication using Monte Carlo procedure (Pagani et al. 1999a), which estimated 15% uncertainty for pCO_2 estimates.

Our Miocene CO_2 estimates agree with the results from alternative methods for estimating past CO_2 levels. These include fossil leaf stomatal densities (Royer, Berner, and Beerling 2001), boron isotopes (Pearson and Palmer 2000), and geochemical models (Berner and Kothavala 2001), which all suggest that the Miocene atmosphere contained relatively low and stable CO_2 concentrations.

3.3.6 Paleozoic Studies

Significant problems emerge with this method when applied to the study of climate in more ancient time periods. In particular, the preservation of open-

ocean sediments decreases back in time, such that Jurassic and older sediments are rare or nonexistent. For Paleozoic reconstructions, workers are required to use sediment samples from ancient epicontinental seas. Constraining nutrient concentrations in the ancient shallow seas is difficult, due to regional variations in the influences from land runoff, restrictions in circulation, and the sensitivity of the shallow waters to relative changes in sea level. Thus it is a significant understatement to claim that precise reconstruction of very ancient CO_2 using phytoplankton organic materials is challenging. Researchers must employ as many localities as possible in order to document and account for the influence of environmental dynamics of individual localities. Interpretation of these records should be done with caution because of the environmental challenges noted above. In addition, our knowledge of phytoplankton carbon assimilation properties is limited for these ancient times. There are few, if any, studies of the controls on isotopic fractionation by phytoplankton groups that dominated the pre-Mesozoic seas, such at the green algae and cyanobacteria. On top of these challenges, the error curves shown in Fig. 3.6 and Fig. 3.7 demonstrate a rapid increase in uncertainty at higher values of ε_p. For times when CO_2 was presumably much higher than the current level (Berner and Kothavala 2001; Rothman 2002), uncertainties in this approach will likely make it unreasonable for reconstruction of absolute CO_2 values, although they can be used to demonstrate very high levels of CO_2 at any particular time.

Nevertheless, records of organic materials isotopic composition can be used to constrain CO_2 levels associated with climate change recorded in sediments, even though precise estimates of CO_2 levels are impossible. For example, the pattern of sedimentary inorganic and organic carbon isotopic excursions can reveal sensitivity of phytoplankton isotopic fraction to CO_2 changes and therefore identify if CO_2 was above a given threshold for sensitivity. For example, if $\delta^{13}C$ values for organic and inorganic carbon track each other, such that ε_p values do not vary across an interval of climatic shift, it suggests that CO_2 levels were high and that phytoplankton were not carbon limited (Kump and Arthur 1999). For example, in the late Frasnian, despite strong evidence for significant carbon burial events and resulting climate change, $\delta^{13}C$ values of phytoplankton biomarkers tracked the inorganic carbon record precisely, suggesting high CO_2 levels during the middle to upper Devonian (Joachimski et al. 2001). This observation does not address the role of CO_2 changes in climate during the isotopic excursion. However, it does help constrain our understanding of CO_2 levels for this time period, and it suggests they were relatively high.

In contrast, for the late middle Ordovician, isotopic values for organic carbon change by several ‰ more than inorganic carbon during a interval of pronounced oceanic cooling. This produced a shift in ε_p values and Patzkowsky et al. (1997) and Pancost, Freeman, and Patzkowsky (1999) have argued this represents a time when CO_2 was at a low enough level that phytoplankton isotopic fractionation was sensitive to changing environmental conditions. If modern algae (i.e., those studied by Popp et al. 1998) are accurate analogs for Paleozoic marine phytoplankton, the CO_2 threshold is approximately 8 to 10 times current

atmospheric level. Thus isotopic data suggests atmospheric CO_2 was above this level in the late Devonian, and below this level in the late Ordovician.

Hayes et al. (1999) compiled inorganic and organic isotopic data in order to constrain CO_2 variations over the past 800 million years. Unlike Pancost et al. (1999) or Joachimski et al. (2001), their reconstructions are based on a compilation of bulk organic carbon analyses as a proxy for phytoplankton isotopic values. Additional caution is needed if bulk organic materials are used because of the potential for mixed signatures from phytoplankton, microorganisms, or other sources of organic carbon (Hayes et al. 1989). Nonetheless, this work extends previous studies (i.e., Popp et al. 1989) and affirms that ε_p has varied significantly over Earth's history.

3.4 Summary

The reconstruction of CO_2 values based on biomarker and isotopic analyses provides many challenges and as many opportunities. The method is best applied when CO_2 levels were relatively low, when phosphate concentrations can be constrained, and with multiple sample localities representing stable oceanographic regimes. With our currently available understanding of alkenone isotopic biogeochemistry and under the best of circumstances, this will lead to uncertainties of approximately 20%. The relative utility of this information depends entirely on the question being addressed. It is inappropriate to expect precise reconstructions on very long timescales because the quality of our understanding of ancient oceanic and biological processes diminishes back in time, while the uncertainty increases at times of high CO_2. However, isotopic variations do record information about very ancient CO_2. Observed variations in e_p can be used to suggest relative changes in CO_2 and whether levels were above or below a threshold level of sensitivity for isotopic fractionation during carbon fixation. Elevated ε_p values approaching the maximum values are associated with significant uncertainty, although when constrained by phosphate estimates, they nonetheless indicate elevated CO_2 levels sufficient to result in the expression of maximum fractionation by enzymatic fixation. In such situations, it is especially necessary to establish multiple records from both high and low phosphate environments to reduce the uncertainty and constrain the range of surface water CO_2 concentrations.

For Cenozoic and potentially late Mesozoic time periods, this approach has valid utility in reconstructing relative changes in CO_2. However, reconstruction of absolute values requires caution, along with the right sample set where the relative influence of nutrient dynamics can be estimated. If a reliable proxy for either nutrient abundances or growth rated becomes available, then researchers will be able to address a fuller range of paleoceanographic and paleoclimate questions than is currently possible. For this approach to be applied with greater confidence on longer timescales, much more work is needed with modern organisms that can serve as analogs for Paleozoic phytoplankton.

Acknowledgments. We thank the National Science Foundation for support of research discussed in this work. K.H. Freeman thanks T. Eglinton, J. Hayes, and the Woods Hole Oceanographic Institution for hosting her sabbatical visit and providing a stimulating environment for the writing of this manuscript.

References

Berner, R.A., and Z. Kothavala. 2001. GEOCARB III: A revised model of atmospheric CO_2 over phanerozoic time. *American Journal of Science* 301:182–204.

Bevington, P.R., and D.K. Robinson. 1992. *Data Reduction and Error Analysis*. New York: McGraw-Hill.

Bidigare, R.R., A. Fluegge, K.H. Freeman, K.L. Hanson, J.M. Hayes, D. Hollander, J.P. Jasper, L.L. King, E.A. Laws, J. Milder, F.J. Millero, R. Pancost, B.N. Popp, P.A. Steinberg, and S.G. Wakeham. 1997. Consistent fractionation of C-13 in nature and in the laboratory: Growth-rate effects in some haptophyte algae. *Global Biogeochemical Cycles* 11:279–92.

———. 1999. Consistent fractionation of C-13 in nature and in the laboratory: Growth-rate effects in some haptophyte algae (1997, 11:279). *Global Biogeochemical Cycles* 13:251–52.

Bidigare, R.R., K.L. Hanson, K.O. Buesseler, S.G. Wakeham, K.H. Freeman, R.D. Pancost, F.J. Millero, P. Steinberg, B.N. Popp, M. Latasa, M.R. Landry, and E.A. Laws. 1999b. Iron-stimulated changes in C-13 fractionation and export by equatorial Pacific phytoplankton: Toward a paleogrowth rate proxy. *Paleoceanography* 14:589–95.

Boyle, E.A. 1992. Cadmium and $\delta^{13}C$ paleochemical ocean distributions during the stage-2 glacial maximum. *Annual Review of Earth and Planetary Science* 20:245–87.

Brassell, S.C. 1993. Applications of biomarkers for delineating marine paleoclimatic fluctuations during the Pleistocene. In *Organic geochemistry: Principles and applications,* ed. M.H. Engel and S.A. Macko, 699–738. New York: Plenum Press.

Brassell, S.C., G. Eglinton, I.T. Marlowe, U. Pflaumann, and M. Sarnthein. 1986. Molecular stratigraphy: A new tool for climatic assessment. *Nature* 320:129–33.

Burkhardt, S., U. Riebesell, and I. Zondervan. 1999. Effects of growth rate, CO_2 concentration, and cell size on the stable carbon isotope fractionation in marine phytoplankton. *Geochimica Et Cosmochimica Acta* 63:3729–41.

Eek, M.K., M.J. Whiticar, J.K.B. Bishop, and C.S. Wong. 1999. Influence of nutrients on carbon isotope fractionation by natural populations of Prymnesiophyte algae in NE Pacific. *Deep-sea research part Ii-topical studies in oceanography* 46:2863–76.

Farquhar, G.D., J.R. Ehleringer, and K.T. Hubick. 1989. Carbon isotope discrimination and photosynthesis. Annual Review of Plant Physiology and Molecular Biology **40**: 503-537.

Francois, R., M.A. Altabet, R. Goericke, D.C. McCorkle, C. Brunet, and A. Poisson. 1993. Changes in the $\delta^{13}C$ of surface-water particulate organic-matter across the subtropical convergence in the SW Indian Ocean. *Global Biogeochemical Cycles* 7:627–44.

Freeman, K.H. 2001. Isotopic biogeochemistry of marine carbon. In *Stable isotope geochemistry,* ed. J.W. Valley and D.R. Cole. Reviewed in *Mineralogy and Geochemistry* 43:579–605.

Freeman, K.H., and J.M. Hayes. 1992. Fractionation of carbon isotopes by phytoplankton and estimates of ancient CO_2 levels. *Global Biogeochem Cycles* 6:185–98.

Freeman, K.H., and S.G. Wakeham. 1992. Variations in the distributions and isotopic compositions of alkenones in Black Sea particles and sediments. *Organic Geochemistry* 19:277–85.

Gong, C., and D.J. Hollander. 1999. Evidence for differential degradation of alkenones

under contrasting bottom water oxygen conditions: Implication for paleotemperature reconstruction. *Geochimica et Cosmochimica Acta* 63:405–11.

Guy, R.D., M.L. Fogel, and J.A. Berry. 1993. Photosynthetic fractionation of the stable isotopes of oxygen and carbon. *Plant Physiology* 101:37–47.

Hayes, J.M. 1993. Factors controlling ^{13}C contents of sedimentary organic compounds-principles and evidence. *Marine Geology* 113:111–25.

———. 2001. Fractionation of carbon and hydrogen isotopes in biosynthetic processes. In *Stable Isotope Geochemistry,* ed. J.W. Valley and D.R. Cole. Reviewed in *Mineralogy and Geochemistry* 43:225–77.

Hayes, J.M., B.N. Popp, R. Takigiku, and M.W. Johnson. 1989. An isotopic study of biogeochemical relationships between carbonates and organic carbon in the Greenhorn Formation. *Geochimica et Cosmochimica Acta* 53:2961–72.

Hayes, J.M., H. Strauss, and A.J. Kaufman. 1999. The abundance of ^{13}C in marine organic matter and isotopic fractionation in the global biogeochemical cycle of carbon during the past 800 Ma. *Chemical Geology* 161:103–25.

Herbert, T.D. 2001. Review of alkenone calibrations (culture, water column, and sediments). *Geochemistry Geophysics Geosystems* 2:2000GC000055.

Hinga, K.R., M.A. Arthur, M.E.Q. Pilson, and D. Whitaker. 1994. Carbon-isotope fractionation by marine phytoplankton in culture: The effects of CO_2 concentration, pH, temperature, and species. *Global Biogeochemical Cycles* 8:91–102.

Jasper, J.P., J.M. Hayes, A.C. Mix, and F.G. Prahl. 1994. Photosynthetic fractionation of ^{13}C and concentrations of dissolved CO_2 in the Central Equatorial Pacific during the last 255,000 years. *Paleoceanography* 9:781–98.

Joachimski, M.M., C. Ostertag-Henning, R.D. Pancost, H. Strauss, K.H. Freeman, R. Littke, J.S.S. Damste, G. and Racki. 2001. Water column anoxia, enhanced productivity, and concomitant changes in $\delta^{13}C$ and $\delta^{34}S$ across the Frasnian-Famennian boundary (Kowala Holy Cross Mountains/Poland). *Chemical Geology* 175:109–31.

Keller, K., and F.M.M. Morel. 1999. A model of carbon isotopic fractionation and active carbon uptake in phytoplankton. *Marine Ecology-Progress Series* 182:295–98.

Kump, L.R., and M.A. Arthur. 1999. Interpreting carbon-isotope excursions: Carbonates and organic matter. *Chemical Geology* 161:181–98.

Laws, E.A., R.R. Bidigare, and B.N. Popp. 1997. Effect of growth rate and CO_2 concentration on carbon isotopic fractionation by the marine diatom *Phaeodactylum tricornutum. Limnology and Oceanography* 42:1552–60.

Laws, E.A., B.N. Popp, R.R. Bidigare, M.C. Kennicutt, and S.A. Macko. 1995. Dependence of phytoplankton carbon isotopic composition on growth-rate and [CO_2 (aq)]: Theoretical considerations and experimental results. *Geochimica et Cosmochimica Acta* 59:1131–38.

Laws, E.A., B.N. Popp, R.R. Bidigare, U. Riebesell, and S. Burkhardt. 2001. Controls on the molecular distribution and carbon isotopic composition of alkenones in certain haptophyte algae. *Geochemistry Geophysics Geosystems* 2:2000GC000057.

de Leeuw, J.W., F.W. van der Meer, W.I.C. Rijpstra, and P.A. Schenck. 1980. Unusual long-chain ketones of algal origin. In *Advances in organic geochemistry 1979, Proceedings of the ninth international meeting on organic geochemistry, University of Newcastle-Upon-Tyne, U.K., September 1979,* ed. A.G. Douglas and J.R. Maxwell, 211–17. New York: Pergamon.

Marlow, I.T., J.C. Green, A.C. Neal, S.C. Brassell, G. Eglinton, and P.A. Course. 1984. Long chain (n-C_{37}-C_{39}) alkenones in the *Prymnesiophyceae*: Distribution of alkenones and other lipids and their taxanomic significance. *British Phycology Journal* 19:203–16.

Mashiotta, T.A., D.W. Lea, and H.J. Spero. 1997. Experimental determination of cadmium uptake in shells of the planktonic foraminifera Orbulina universa and Globigerina bulloides: Implications for surface water paleoreconstructions. *Geochimica et Cosmochimica Acta* 61:4053–65.

Mook, W.G., J.C. Bommerson, and W.H. Staberman. 1974. Carbon isotope fractionation between dissolved bicarbonate and gaseous carbon dioxide. *Earth and Planetary Science Letters* **22**:169–76.

Nimer, N.A., M.D. Iglesias Rodriguez, and M.J. Merrett. 1997. Bicarbonate utilization by marine phytoplankton species. *Journal of Phycology* 33:625–31.

Ohkouchi, N., K. Kawamura, H. Kawahata, and H. Okada. 1999. Depth ranges of alkenone production in the central Pacific Ocean. *Global Biogeochemical Cycles* 13: 695–704.

Oppo, D.W. and Y. Rosenthal. 1994. Cd/Ca changes in a deep cape basin core over the past 730,000 years: Response of circumpolar deep-water variability to northern-hemisphere ice-sheet melting. *Paleoceanography* 9:661–75.

Pacanowski, R., K. Dixon, and A. Rosati. 1991. *The G.F.D.L. Modular Ocean Model users guide*. NOAA/Geophysical Fluid Dynamics Laboratory.

Pagani, M. 2002. The alkenone-CO_2 proxy and ancient atmospheric carbon dioxide. *Philosophical Transactions of the Royal Society of London Series a—Mathematical Physical and Engineering Sciences* 360:609–32.

Pagani, M., M.A. Arthur, and K.H. Freeman. 2000. Variations in Miocene phytoplankton growth rates in the southwest Atlantic: Evidence for changes in ocean circulation. *Paleoceanography* 15:486–96.

———. 1999. Miocene evolution of atmospheric carbon dioxide. *Paleoceanography* 14: 273–92.

Pagani, M., K.H. Freeman, and M.A. Arthur. 1999. Late miocene atmospheric CO_2 concentrations and the expansion of C_4 grasses. *Science* 285:876–79.

Pagani, M., K.H. Freeman, N. Ohkouchi, and K. Caldeira. 2002. Comparison of water column [CO_2aq] with sedimentary alkenone-based estimate: A test of the alkenone-CO_2 proxy. *Paleoceanography* 17:1069–81.

Pancost, R.D., K.H. Freeman, and M.E. Patzkowsky. 1999. Organic-matter source variation and the expression of a late middle Ordovician carbon isotope excursion. *Geology* 27:1015–18.

Pancost, R.D., K.H. Freeman, S.G. Wakeham, and C.Y. Robertson. 1997. Controls on carbon isotope fractionation by diatoms in the Peru upwelling region. *Geochimica et Cosmochimica Acta* 61:4983–91.

Patzkowsky, M.E., L.M. Slupik, M.A. Arthur, R.D. Pancost, and K.H. Freeman. 1997. Late middle Ordovician environmental change and extinction: Harbinger of the late Ordovician or continuation of Cambrian patterns? *Geology* **25**:911–14.

Pearson, P.N., and M.R. Palmer. 2000. Atmospheric carbon dioxide concentrations over the past 60 million years. *Nature* **406**:695–99.

Popp, B.N., E.A. Laws, R.R. Bidigare, J.E. Dore, K.L. Hanson, and S.G. Wakeham. 1998. Effect of phytoplankton cell geometry on carbon isotopic fractionation. *Geochimica et Cosmochimica Acta* 62:69–77.

Popp, B.N., R. Takigiku, J.M. Hayes, J.W. Louda, and E.W. Baker. 1989. The post-Paleozoic chronology and mechanism of ^{13}C depletion in primary marine organic matter. *American Journal of Science* 289:436–54.

Popp, B.N., T. Trull, F. Kenig, S.G. Wakeham, T.M. Rust, B. Tilbrook, F.B. Griffiths, S.W. Wright, H.J. Marchant, R.R. Bidigare, and E.A. Laws. 1999. Controls on the carbon isotopic composition of Southern Ocean phytoplankton. *Global Biogeochemical Cycles* 13:827–43.

Rau, G.H., U. Riebesell, and D. Wolf-Gladrow. 1996. A model of photosynthetic ^{13}C fractionation by marine phytoplankton based on diffusive molecular CO_2 uptake. *Marine Ecology-Progress Series* 133:275–85.

Rau, G.H., T. Takahashi, D.J. Desmarais, D.J. Repeta, and J.H. Martin. 1992. The relationship between $\delta^{13}C$ of organic matter and [CO_2(aq)] in ocean surface-water data from a JGOFS site in the Northeast Atlantic Ocean and a model. *Geochimica et Cosmochimica Acta* 56:1413–19.

−1
0
+1

Rechka, J.A., and J.R. Maxwell. 1988a. Characterization of alkenone temperature indicators in sediments and organisms. *Organic Geochemistry* 13:727–34.

———. 1988b. Unusual long-chain ketones of algal origin. *Tetrahedron Letters* 29:2599–2600.

Rickaby, R.E.M., and H. Elderfield. Planktonic formainiferal Cd/Ca: Paleonutrients or paleotemperature? *Paleoceanography* 14:293–303.

Riebesell, U., S. Burkhardt, A. Dauelsberg, and B. Kroon. 2000a. Carbon isotope fractionation by a marine diatom: Dependence on the growth-rate-limiting resource. *Marine Ecology-Progress Series* 193:295–303.

Riebesell, U., A.T. Revill, D.G. Holdsworth, and J.K. Volkman. 2000b. The effects of varying CO_2 concentration on lipid composition and carbon isotope fractionation in Emiliania huxleyi. *Geochimica et Cosmochimica Acta* 64:4179–92.

Roeske, C.A., and M.H. O'Leary. 1985. Carbon isotope effect on carboxylation of ribulose bisphosphate carboxylase from *Rhodospirillum rubum. Biochemistry* **24**:1603–607.

Romanek, C.S., E.L. Grossman, and J.W. Morse. 1992. Carbon isotopic fractionation in synthetic aragonite and calcite—effects of temperature and precipitation rate *Geochimica et Cosmochimica Acta* 56:419,430.

Rosenthal, Y., H. Stoll, K. Wyman, and P.G. Falkowski. 1999. Growth related variations in carbon isotopic fractionation and coccolith chemistry in Emiliania huxleyi. *EOS Trans., Ocean Science Meeting Supplement* 80(90), OS11C-27.

Rothman, D.H. 2002. Atmospheric carbon dioxide levels for the last 500 million years. *Proceedings of the National Academy of Sciences* 99:4167–171.

Royer, D.L., R.A. Berner, and D.J. Beerling. 2001. Phanerozoic atmospheric CO_2 change: Evaluating geochemical and paleobiological approaches. *Earth-Science Reviews* 54: 349–92.

Sachs, J.P., and S.J. Lehman. 1999. Subtropical North Atlantic temperatures 60,000 to 30,000 years ago. *Science* 286:756–59.

Schouten, S., W. Breteler, P. Blokker, N. Schogt, W.I.C. Rijpstra, K. Grice, M. Baas, and J.S.S. Damste. 1998. Biosynthetic effects on the stable carbon isotopic compositions of algal lipids: Implications for deciphering the carbon isotopic biomarker record. *Geochimica et Cosmochimica Acta* 62:1397–1406.

Sharkey, T.D., and J.A. Berry. Carbon isotope fractionation of algae as influenced by an inducible CO_2 concentrating mechanism. In *Inorganic carbon uptake by aquatic photosynthetic organisms,* ed. W.J. Lucas and J.A. Berry, 389–401. Rockville, Md: American Society of Plant Physiologists.

Sikes, C.S., R.D. Roer, and K.M. Wilbur. 1980. Photosynthesis and coccolith formation: Inorganic carbon sources and net inorganic reaction of deposition. *Limnology and Oceanography* 25:248–61.

Spero, H.J., and M.J. Deniro. 1987. The influence of symbiont photosynthesis on the $\delta^{18}O$ and $\delta^{13}C$ values of planktonic foraminiferal shell calcite. *Symbiosis* 4:213–28.

Spero, H.J., and D.W. Lea. 1993. Intraspecific stable-isotope variability in the planktic foraminifera *Globigerinoides sacculifer*: Results from laboratory experiments. *Marine Micropaleontology* 22:221–34.

Sokal, R.R., and F.J. Rohlf. 1995. *Biometry*. New York: W.H. Freeman.

Taylor, J.R. 1982. *An Introduction to Error Analysis*. University Science Books, Mill Valley, CA.

Verity, P.G., C.Y. Robertson, C.R. Tronzo, M.G. Andrews, J.R. Nelson, and M.E. Sieracki. 1992. Relationships between cell-volume and the carbon and nitrogen content of marine photosynthetic nanoplankton. *Limnology and Oceanography* 37:1434–46.

Volkman, J.K., S.M. Barrett, S.I. Blackburn, and E.L. Sikes. 1995. Alkenones in *Gephyrocapsa oceanica*: Implications for studies of paleoclimate. *Geochimica et Cosmochimica Acta* 59:513–20.

Volkman, J.K., G. Eglinton, E.D. Corner, and J.R. Sargent. 1980. Novel unsaturated

straight-chain C37–C39 methyl and ethyl ketones in marine sediments and a coccolithophore Emiliania huxleyi. In *Advances in organic geochemistry 1979; Proceedings of the ninth international meeting on organic geochemistry, University of Newcastle-Upon-Tyne, U.K., September 1979,* ed. A.G. Douglas and J.R. Maxwell, 219–27. New York: Pergamon.

Wakeham, S.G., J.I. Hedges, C. Lee, M.L. Peterson, and P.J. Hernes. 1997a. Compositions and transport of lipid biomarkers through the water column and surficial sediments of the equatorial Pacific Ocean. *Deep-Sea Research Part II-Topical Studies in Oceanography* 44:2131–62.

Wakeham, S.G., C. Lee, J.I. Hedges, P.J. Hernes, and M.L. Peterson. 1997b. Molecular indicators of diagenetic status in marine organic matter. *Geochimica et Cosmochimica Acta* 61:5363–69.

Wakeham, S.G., M.L. Peterson, J.I. Hedges, and C. Lee. 2002. Lipid biomarker fluxes in the Arabian Sea, with a comparison to the equatorial Pacific Ocean. *Deep-Sea Research Part Ii-Topical Studies in Oceanography* 49:2265–2301.

Westbroek, P., C.W. Brown, J. Vanbleijswijk, C. Brownlee, G.J. Brummer, M. Conte, J. Egge, E. Fernandez, R. Jordan, M. Knappertsbusch, J. Stefels, M. Veldhuis, P. Vanderwal, and J. Young. 1993. A model system approach to biological climate forcing: The example of *Emiliania huxleyi*. *Global and Planetary Change* 8:27–46.

−1
0
+1

James R. Ehleringer Thure E. Cerling
M. Denise Dearing
Editors

A History of Atmospheric CO_2 and Its Effects on Plants, Animals, and Ecosystems

With 161 Illustrations

Springer

James R. Ehleringer
Department of Biology
University of Utah
Salt Lake City, UT 84112
USA

Thure E. Cerling
Department of Geology and Geophysics
Department of Biology
University of Utah
Salt Lake City, UT 84112 USA

M. Denise Dearing
Department of Biology
University of Utah
Salt Lake City, UT 84112
USA

Cover illustration: A plot of the environmental and ecological factors that govern shifts in the abundances of C_3 monocots and C_4 dicots within grassland and savanna ecosystems.

ISSN 0070-8356
ISBN 0-387-22069-0 e-ISBN <to come> Printed on acid-free paper.

Printed in the United States of America. (WBG/MVY)

9 8 7 6 5 4 3 2 1 SPIN 10940464

Springer is a part of Springer Science+Business Media
springeronline.com